Supporting Information

NIR-II Fluorescent Molecular Bottlebrush Prepared by Ring-opening Polymerization for Programmed Cell Death Ligand-1 Checkpoint Imaging

Chao Wang,[†] *Pengfei Sun,*[*,†] *Quli Fan,*[*,†] *and Wei Huang*[‡]

†State Key Laboratory of Organic Electronics and Information Displays & Institute of Advanced Materials (IAM), Nanjing University of Posts & Telecommunications, 9 Wenyuan Road, Nanjing 210023, China

‡Frontiers Science Center for Flexible Electronics (FSCFE), MIIT Key Laboratory of Flexible Electronics (KLoFE), Northwestern Polytechnical University, Xi'an 710072, China

***Pengfei Sun**. Email: iampfsun@njupt.edu.cn

***Quli Fan.** Email: iamqlfan@njupt.edu.cn

Materials. TTQ and F-B were purchased from SunaTech Inc. (China). Lys(Tfa)-NCA and Glu(Obzl)-NCA were purchased from Nanjing Chemlin Chemical Industry Co., Ltd. (China). CT-26 colon cancer cells, 4T1 murine breast cancer cells, PD-L1 mAb and dulbecco's modified eagle medium (DMEM) were purchased from KeyGEN BioChemical Technology Co., Ltd.(China). Other reagents were purchased from Shanghai J&K Scientific Co., Ltd. (China) and Shanghai Macklin Biochemical Technology Co., Ltd.(China).

Characterization. The spectra of ^{1}H NMR were obtained on a Bruker Ultra Shield Plus 400 MHz NMR spectrometer at 20.0˚C. Molecular weight and distribution measurements were conducted using gel permeation chromatography (GPC) equipped with the RID1A, Refractive Index Signal detector. Transmission electron microscopy (TEM) images were collected on a HT7700 transmission electron microscope. The TEM specimens were made on a carbon-coated copper grid via placing a drop of simple. Dynamic light scattering (DLS) analyze was obtained by an ALV/CGS-3 light scattering spectrometer equipped with a laser of He-Ne (wavelength = 632.8 nm) and an ALV-7004 multi-τ digital time correlator. A CONTIN analysis, from the scattering intensity, served to extract the $<D_h>$ data. All test samples were filtrated though Millipore filters (0.45 μm).

The UV-visible (UV-Vis) absorption spectra were achieved by using a UV-Vis-NIR Shimadzu UV-3600 spectrophotometer (Japan). The fluorescence spectra of the nanoparticles in the NIR-II region were recorded by using a Fluorolog 3 NIR-II spectroscopy with InGaAs NIR detector under an 808 nm diode laser excitation. The

spectra of fluorescence were further corrected accounting to the detector sensitivity profile after basic emission data acquisition.

NIR-II bioimaging system was installed by Wuhan Grand-imaging Technology Co., Ltd. (China) and a Princeton thermoelectric cooled two-dimensional InGaAs camera was used to record *in vivo* and *in vitro* NIR-II fluorescence imaging. The excitation light was an 808 nm diode laser (40 mW/cm^2), and the emission light was detected through a 50 mm camera lens equipped with 1,064 nm long pass filers as required.

Tumor model. All the animal experiments of this research were performed in strict accordance with The National Regulation of China for Care and Use of Laboratory Animals, and the protocol was approved by the Jiangsu Administration of Experimental Animals. For the target experiment, tumor models in BALB/c mice were established by orthotopically injecting CT26 or 4T1 cells (1×10^6) into the back of each mouse. All the animals were purchased from KeyGEN Bio TECH (China).

NIR-II imaging of PD-L1. For *in vivo* immune checkpoint PD-L1 imaging, the NIR-II imaging system with 1064 nm long pass (LP) filter was used to get NIR-II fluorescence image of mice under the exposure time of 1,000 ms upon an 808-nm laser excitation. The software of the NIR-II imaging system can optimize the NIR-II images. Before the imaging, 150 μL of (anti-PD-L1)-P(TTQ-F)-g-(PLL_{30}-g-$(PGA)_5$) PBS solution (3 mg/mL) and P(TTQ-F)-g-(PLL_{30}-g-$(PGA)_5$) PBS solution (3 mg/mL) were injected into mice bearing CT26 tumor through tail vein, respectively. Then 150 μL of (anti-PD-L1)-P(TTQ-F)-g-(PLL_{30}-g-$(PGA)_5$) PBS solution (3 mg/mL) was injected into mice bearing 4T1 tumor through tail vein. NIR-II images of mice were collected

at various time points p.i.. These mice were sacrificed at 24 h post injection, and their hearts, livers, spleens, lungs, kidneys and tumor tissues harvested for *ex vivo* imaging.

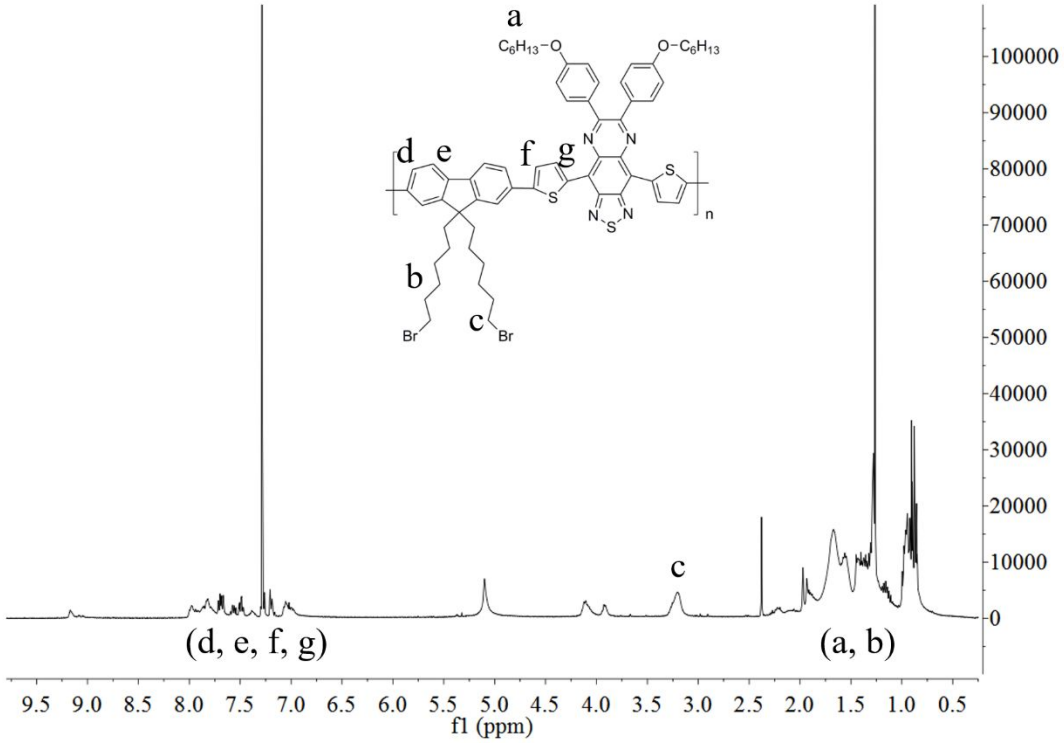

Figure S1 ^{1}H NMR spectrum of P(TTQ-F) in methyl sulfoxide-d6.

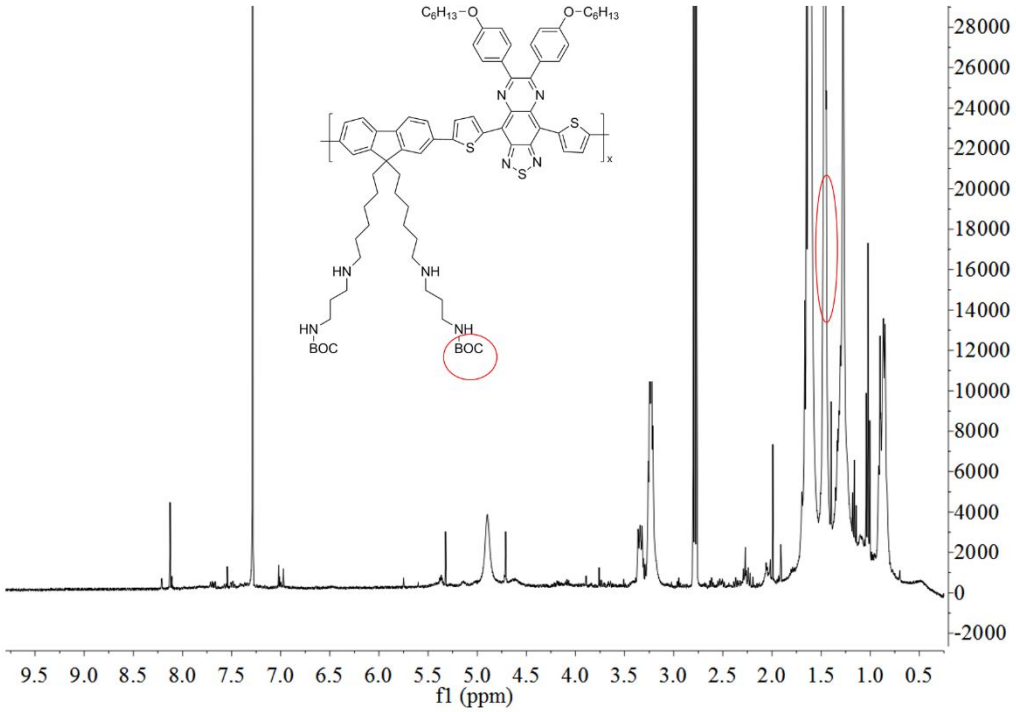

Figure S2 ^{1}H NMR spectrum of P(TTQ-F-NH(BOC)) in methyl sulfoxide-d6.

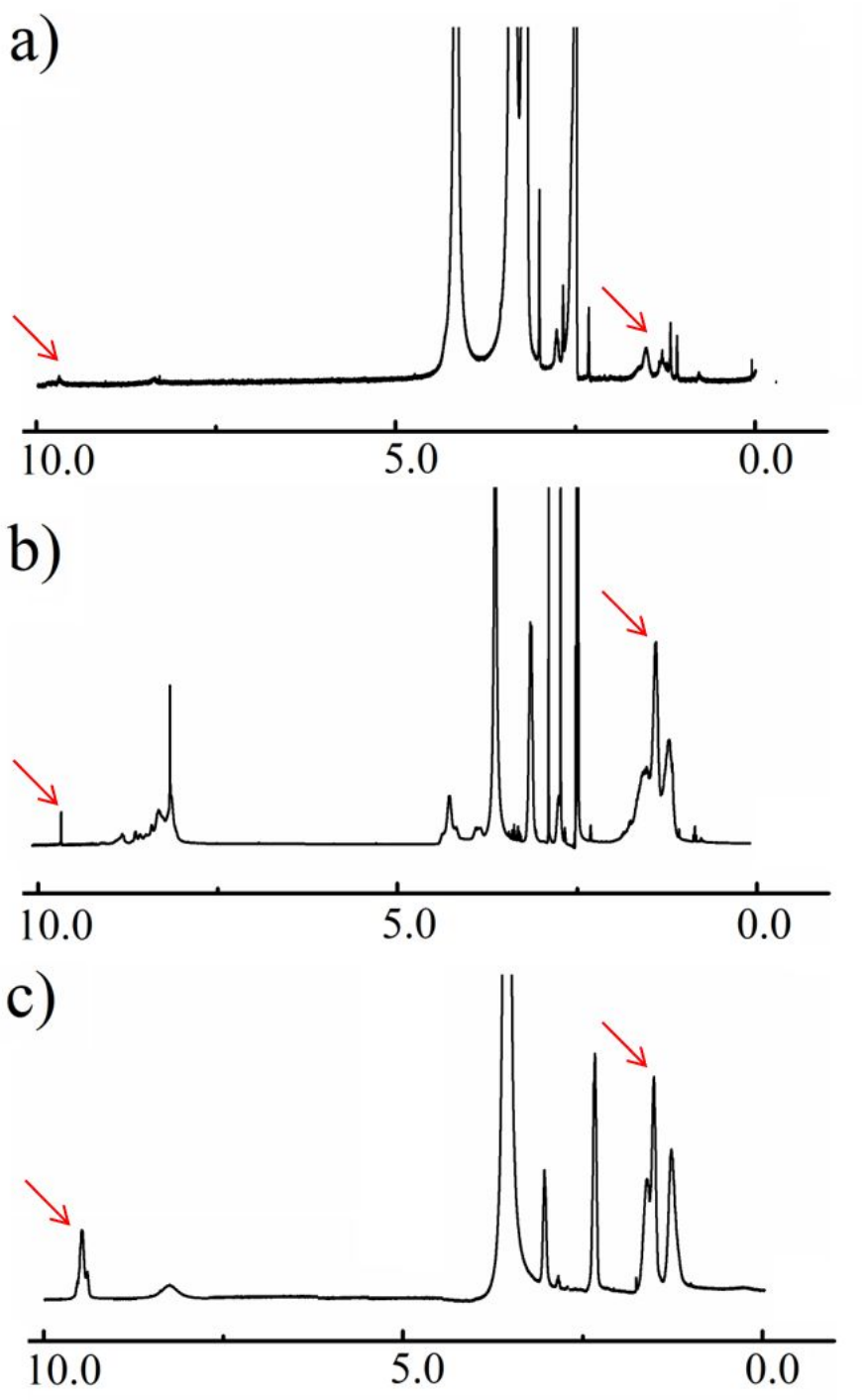

Figure S3 ^{1}H NMR spectrum of P(TTQ-F)-g-$(PLL)_{20}$ (a), P(TTQ-F)-g-$(PLL)_{30}$ (b), and P(TTQ-F)-g-$(PLL)_{50}$ (c) in methyl sulfoxide-d6 (the red arrows indicate the peak of PLL).

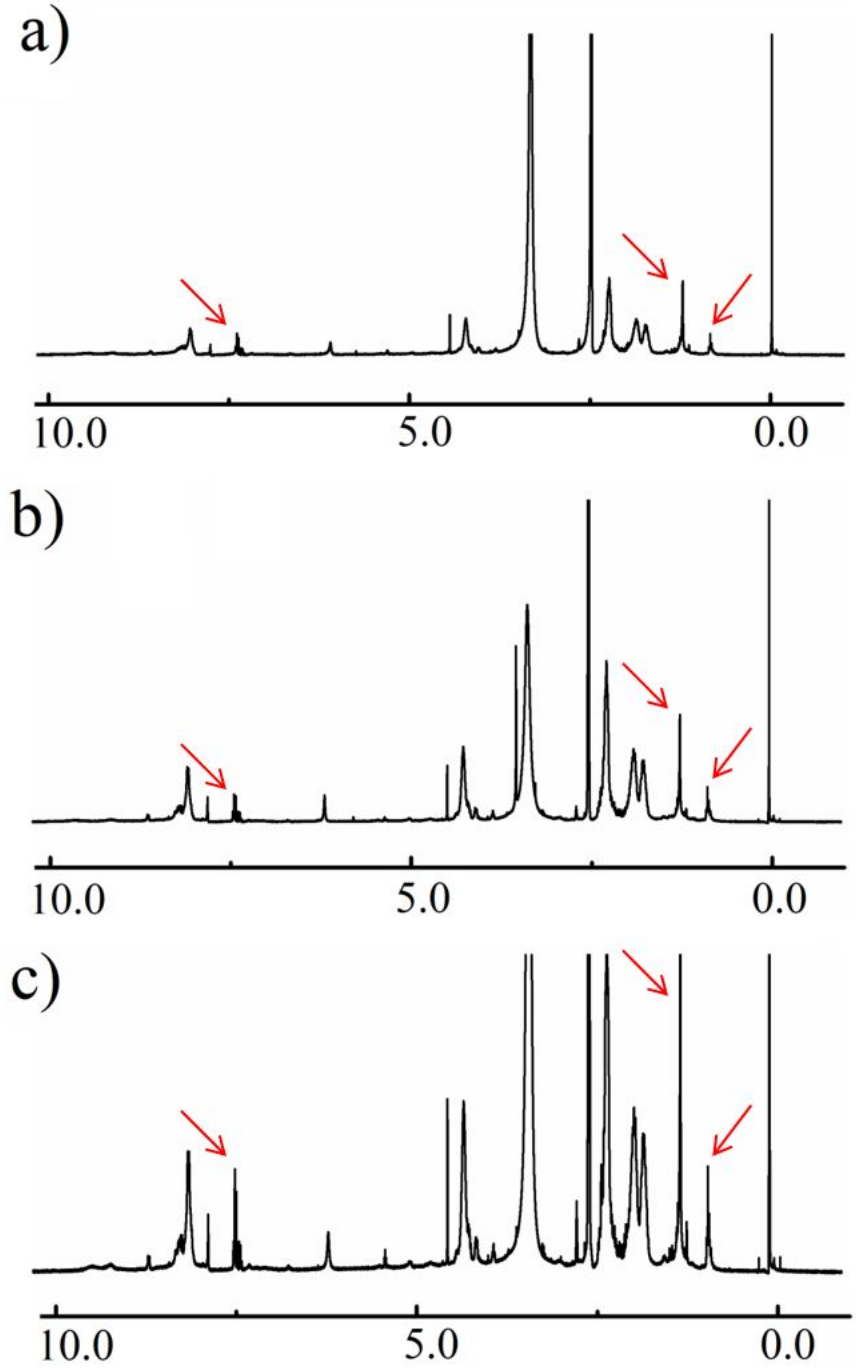

Figure S4 ^{1}H NMR spectrum of P(TTQ-F)-g-(PLL_{20}-g-$(PGA)_5$) (a), P(TTQ-F)-g-(PLL_{30}-g-$(PGA)_5$) (b), and P(TTQ-F)-g-(PLL_{50}-g-$(PGA)_5$) (c) in methyl sulfoxide-d6 (the red arrows indicate the peak of PGA).

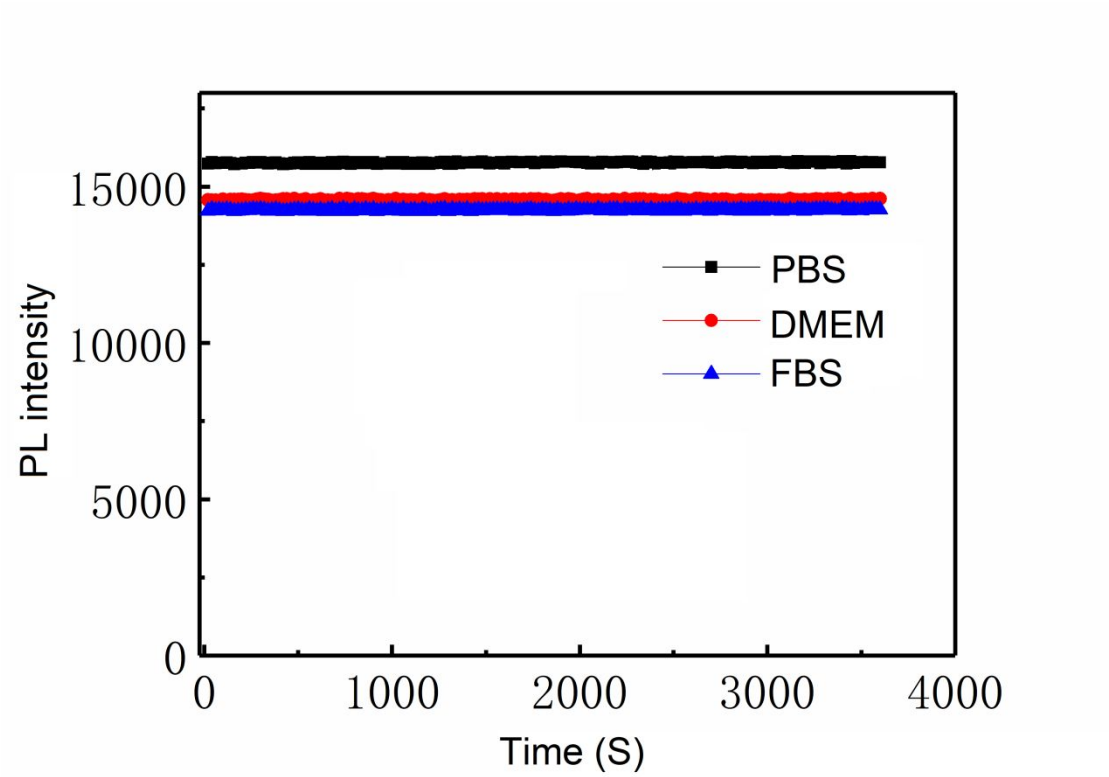

Figure S5 The photostability of P(TTQ-F)-g-(PLL_{30}-g-$(PGA)_5$) in PBS, DMEM and FBS under a continuous 808 nm laser at a power density of 0.5 W/cm^2.

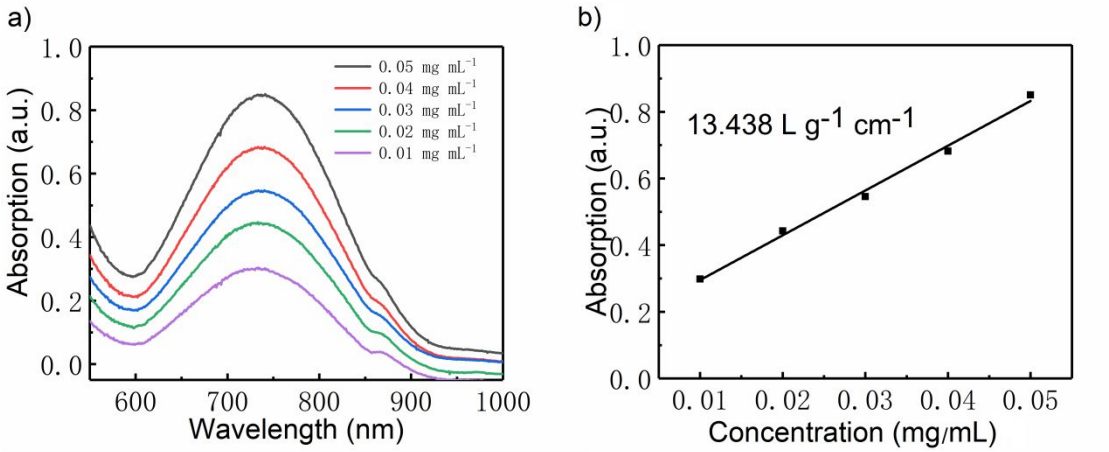

Figure S6 (a) UV spectrum of P(TTQ-F)-g-(PLL_{30}-g-$(PGA)_5$) in water at different concentrations. (b) Absorption coefficient at maximum absorption peak.

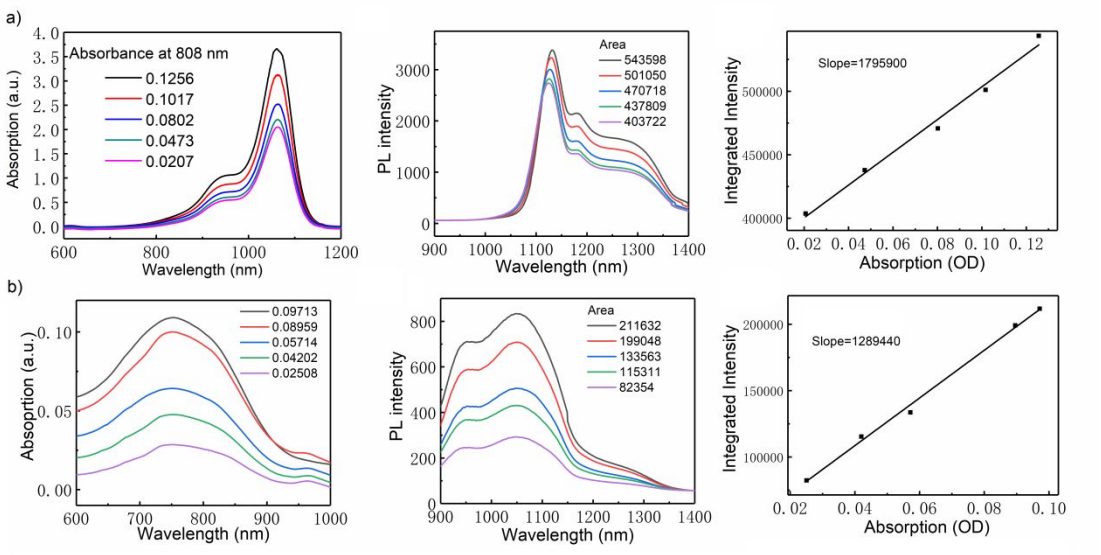

Figure S7 Quantum yield measurement of P(TTQ-F)-g-(PLL$_{30}$-g-(PGA)$_5$) with IR 1061 as the reference sample. Absorption and fluorescence emission spectra of IR1061 in DCM (a) and P(TTQ-F)-g-(PLL$_{30}$-g-(PGA)$_5$) (b) in water.

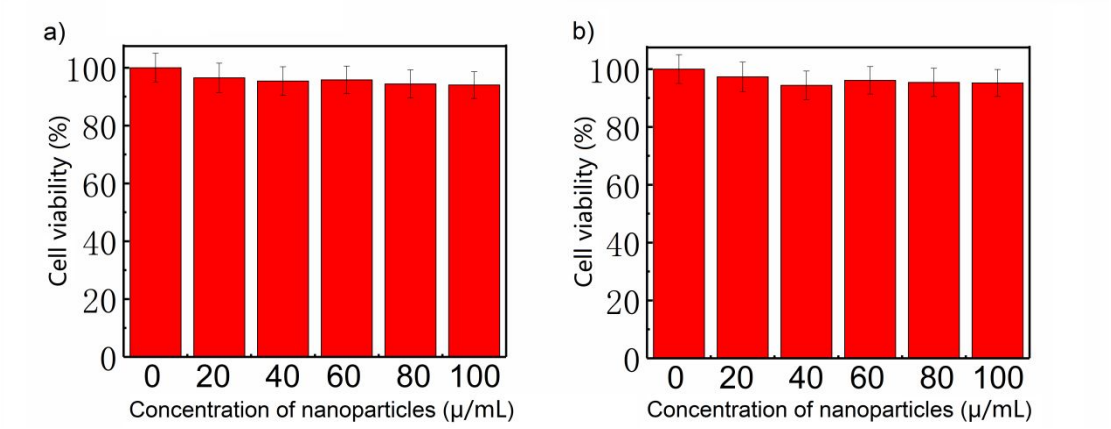

Figure S8 CT26 (a) and 4T1 (b) Cells viability under different concentrations (0−100 μg/mL) of (anti-PD-L1)-P(TTQ-F)-g-(PLL$_{30}$-g-(PGA)$_5$) for 24 h.

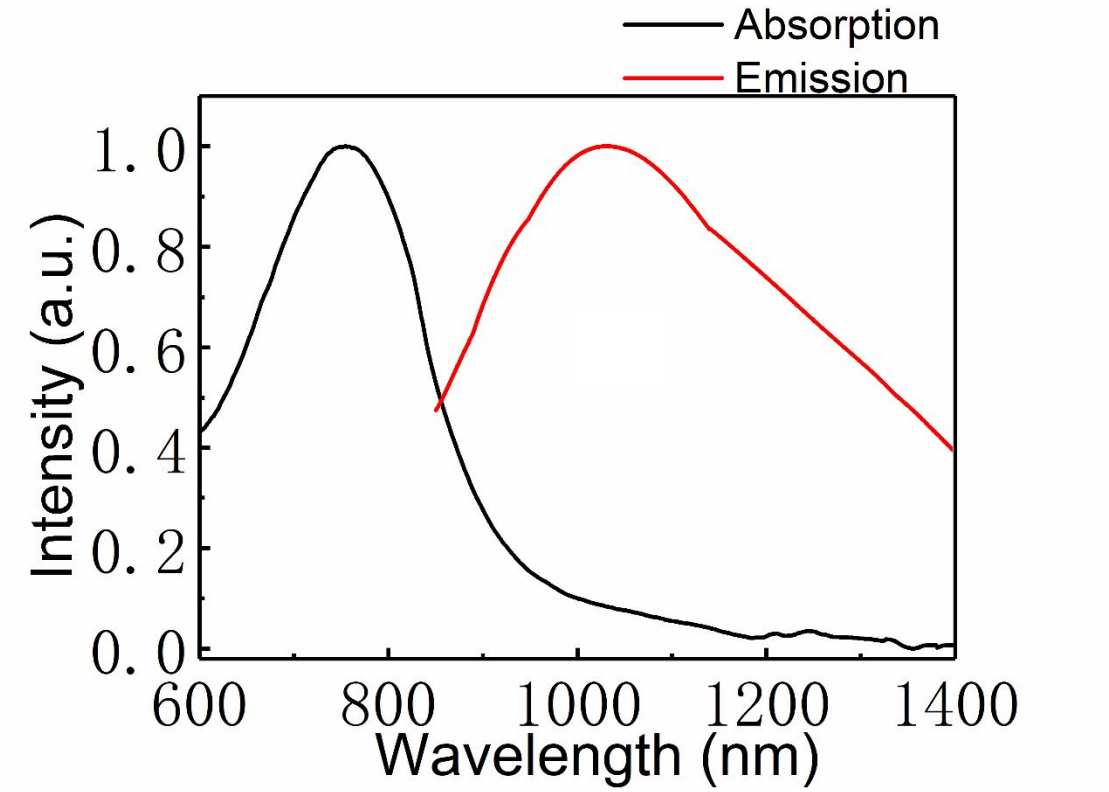

Figure S9 UV spectrum of (anti-PD-L1)-P(TTQ-F)-g-(PLL_{30}-g-$(PGA)_5$) (black) and fluorescence spectrum of P(TTQ-F-NH2) (red).

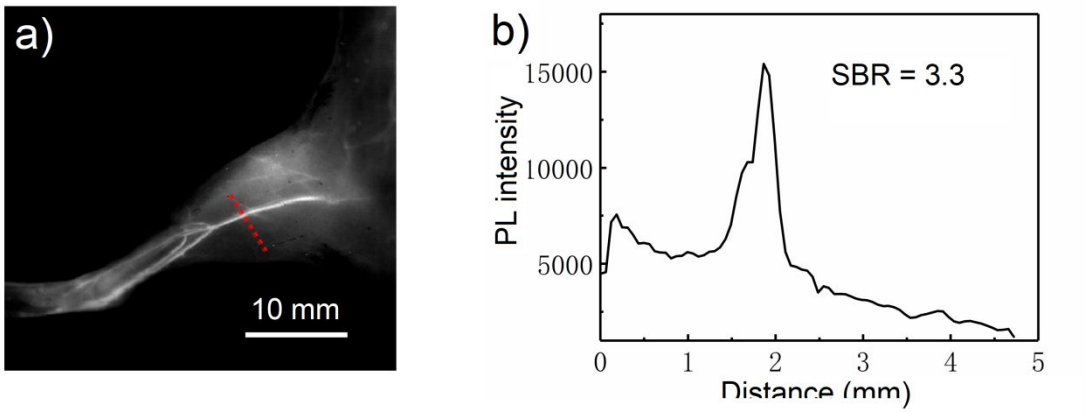

Figure S10 Fluorescence image of the vasculature of the hind limb in nude mice with (anti-PD-L1)-P(TTQ-F)-g-(PLL_{30}-g-$(PGA)_5$) is shown in (a), with cross-sectional fluorescent intensity profiles of red dotted lines and the vessel intensity analysis (b).